

Glueball nature of the $\sigma/f_0(600)$ from $\pi\pi$ and $\gamma\gamma$ scatterings

G. Mennessier* ^a, S. Narison† ^a, and W. Ochs‡ ^b

^aLaboratoire de Physique Théorique et Astroparticules, Université de Montpellier II, Case 070, Place Eugène Bataillon, 34095 - Montpellier Cedex 05, France

^bMax-Planck Institut für Physik, D 80805 Munich, Föhringer Ring 6, Germany,

We estimate the $I = 0$ scalar meson $\sigma/f_0(600)$ parameters from $\pi\pi$ and $\gamma\gamma$ scattering data below 700 MeV using an improved analytic K-matrix model. A fit of the hadronic data gives a complex pole mass $M_\sigma = 422 - i 290$ MeV, while simultaneous best fits of the $\gamma\gamma \rightarrow \pi^+\pi^-$, $\pi^0\pi^0$ data give a direct width of (0.13 ± 0.05) keV, a rescattering component of (2.7 ± 0.4) keV and a total (direct+rescattering) width of (3.9 ± 0.6) keV. “Running” these results to the physical real axis, the small “direct” $\gamma\gamma$ and the large hadronic widths at the “on-shell” mass are compatible with QCD spectral sum rules (QSSR) and some low-energy theorems (LET) expectations for an unmixed lowest mass glueball/gluonium σ_B of a mass around 1 GeV and a large OZI-violation decay into $\pi\pi$.

1. Introduction

Understanding the nature of scalar mesons in terms of quark and gluon constituents is a long standing puzzle in QCD [1]. One might expect that the decay rate of these mesons into two photons could provide an important information about their intrinsic composite structure. The problem here is that some states are very broad (σ and κ mesons), others are close to an inelastic threshold ($f_0(980)$, $a_0(980)$), which makes their interpretation more difficult. Besides the interpretation within a $q\bar{q}$ model [1,2,3,4,5,6,7] or unitarized quark model [8,9], also the possibility of tetraquark states [10,11,12,13,14] (and some other related scenarios: meson-meson molecules [15,16], meson exchange [17]) is considered. In addition, a gluonic meson is expected in the scalar sector, according to lattice QCD [18,19], QCD spectral sum rules (QSSR) [20,21,22,23,24,4,7] à la SVZ [25,26], and some low-energy theorems (LET) [24,27,28]. Such a state could mix with the other $q\bar{q}$ mesons [3,4,6,29,30]. Among the light particles, the $f_0(600)/\sigma$ meson could be such a gluonic resonance. It can manifest itself in some effective linear sigma models [31,32,33] or contribute to the low-energy constants at $\mathcal{O}(p^4)$ of the QCD effective chiral Lagrangian [34]. Recent analyses of the $\gamma\gamma \rightarrow \pi\pi$ processes have extracted the width of $f_0(600)/\sigma \rightarrow \gamma\gamma$ in the range: (4.1 ± 0.3) keV [35], (3.5 ± 0.7) or (2.4 ± 0.5) keV [36] to (1.8 ± 0.4) keV [37], while the one from nucleon electromagnetic polarizabilities has given (1.2 ± 0.4) keV [38]. Some of these results have been interpreted in [35] as disfavouring a gluonic nature which is expected to have a small coupling to $\gamma\gamma$ [24,3,4,14,16,13]. In the following, we shall reconsider the analysis of the $\gamma\gamma \rightarrow \pi\pi$ process in the low energy region below 700 MeV, where we conclude that it is dominated by the coupling of the photons to charged pions and their rescattering, which therefore can hide any direct coupling of the photons to the scalar mesons. Some first results from this study have been presented in [39].

*Email: gerard.mennessier@lpta.univ-montp2.fr

†Email: snarison@yahoo.fr

‡Email: wwo@mppmu.mpg.de

2. Results suggesting a light 0^{++} glueball

The existence of glueballs/gluonia is a characteristic prediction of QCD and some scenarios have been developed already back in 1975 [40]. Today, there is agreement that such states exist in QCD and the lightest state has quantum numbers $J^{PC} = 0^{++}$.

Lattice QCD - Calculations in the simplified world without quark pair creation (quenched approximation) find the lightest state at a mass around 1600 MeV [18]. These findings lead to the construction of models where the lightest glueball/gluonium mixes with other mesons in the nearby mass range at around (1300-1800) MeV (see, for example, [29]). However, recent results beyond this quenched approximation [19] suggest that the lightest state with a large gluonic component is expected in the region around 1 GeV, and therefore, a scheme based on the mixing of meson states with all masses higher than 1300 MeV could be insufficient to represent the gluonic degrees of freedom in the meson spectrum. Further studies concerning the dependence on lattice spacings and the quark mass appear important.

QSSR and LET - These approaches have given quantitative estimates of the mass of glueballs/gluonia [22, 23,4] and of some essential features of its branching ratios [24,4,7,20,31]. As we shall see in section 5, these approaches require the existence of a gluonium σ_B below 1 GeV having a large $\pi\pi$ but small $\gamma\gamma$ widths, in addition to its corresponding radial excitation σ'_B and a narrow gluonium $G(1.5-1.6)$ coupled weakly to $\pi\pi$ [22,24,4,7].

Phenomenological studies - The identification of the scalar glueball from experiment requires a full understanding of the scalar meson spectrum. After grouping states into flavour multiplets the left over states are candidates for glueballs. Several schemes exist, motivated by the quenched lattice result, where the extra gluonic state is assumed to mix into the three isoscalars $f_0(1370)$, $f_0(1500)$ and $f_0(1710)$ [29]. In an alternative approach [6] (see also ref. [41]) the lightest $q\bar{q}$ multiplet is formed from $f_0(980)$, $f_0(1500)$, $K_0^*(1430)$ and $a_0(1450)$, and the glueball is identified as the broad ob-

ject at smaller mass represented by $f_0(600)$; it dominates $\pi\pi$ scattering near 1 GeV but extends from threshold up to ~ 1800 MeV. The appearance of this broad object in most gluon rich processes was considered in support of this hypothesis. In this analysis of the spectrum, results from elastic and inelastic $\pi\pi$ scattering as well as from D , B and J/ψ decays have been considered [6,42,43].

3. Constraints on $\gamma\gamma$ from $\pi\pi$ processes

Given a set of coupled multi-channel strong processes, related electromagnetic or weak processes are largely predetermined. First, there are the multi-channel extended unitarity relations for the amplitudes with mixed strong and weak couplings (corresponding to the Watson theorem for the single channel); secondly, there are dispersion relations which these amplitudes have to fulfill (though not proved for composite particles). The general consequences of these constraints have been investigated by Omnes and Muskhelishvili [44] for the single- and multi-channel cases. The amplitudes for the weakly coupled processes are largely determined by strong amplitudes, but there are polynomial ambiguities which result from subtraction terms of the dispersion relations depending on the asymptotic high energy behaviour.

The analytic K-matrix model

This general formalism has been applied by Mennessier [45] (see also [46]) to the calculation of the electromagnetic processes $\gamma\gamma \rightarrow \pi\pi, K\bar{K}$, given the strong processes $\pi\pi \rightarrow \pi\pi, K\bar{K}$. The strong processes are represented by a K matrix model representing the amplitudes by a set of resonance poles. In that case, the dispersion relations in the multi-channel case can be solved explicitly, which is not possible otherwise. This model can be reproduced by a set of Feynman diagrams, including resonance (bare) couplings to $\pi\pi$ and $K\bar{K}$ and 4-point $\pi\pi$ and $K\bar{K}$ interaction vertices. A subclass of bubble pion loop diagrams including resonance poles in the s-channel are resummed (unitarized Born). The model also includes contributions from the exchange of vector mesons in the t-channel which become important at the higher energies above 700 MeV. The $\gamma\gamma$ scattering amplitudes also fulfill the constraints at $s = 0$ required by the Born approximation. The radiative width of the resonances cannot be predicted due to the polynomial ambiguity, which can be taken into account by introducing as free parameters the “direct couplings” of the resonances to $\gamma\gamma$ in an effective interaction vertex. In the present analysis we have extended the model by the introduction of a *shape function* which takes explicitly into account left-handed cut singularities for the strong interaction amplitude. This allows a more flexible parametrisation of the $\pi\pi$ data at low energies and improves the high energy behaviour. Next we discuss the features of the model at low and at high energies.

Low energy limit: rescattering

A striking feature of the low energy $\gamma\gamma \rightarrow \pi\pi$ scattering is the dominance of the charged over the neutral $\pi\pi$ cross section by an order of magnitude which can be explained by the contribution of the one-pion-exchange Born term

in $\gamma\gamma \rightarrow \pi^+\pi^-$. In the process $\gamma\gamma \rightarrow \pi^0\pi^0$, the photons cannot couple “directly” to $\pi^0\pi^0$ but through intermediate charged pions and subsequent rescattering with charge exchange. This feature is realized in the analytic model [45]. A similar approach has been applied in the model of Ref. [47] which described data on $\gamma\gamma \rightarrow \pi\pi$ up to 900 MeV by rescattering. A modern example for the importance of rescattering is Chiral perturbation theory. To one-loop accuracy, the calculation based on one pion exchange and $\pi\pi$ rescattering relates the $\gamma\gamma \rightarrow \pi^0\pi^0$ to the $\pi^+\pi^- \rightarrow \pi^0\pi^0$ cross-section using m_π , f_π and e [48]. The 2-loop corrections obtained in [49] includes contributions from other exchanges (spin 1). It amounts to about 30% of the lowest order results and provides a reasonable description of the data up to ~ 700 MeV.

High energy limit: direct production

Whereas at low energy the photon interacts by its coupling to the charged pions, the situation becomes different at high energies where the photon can resolve the constituents of the hadrons. An example is the production of $f_2(1270)$ in $\gamma\gamma \rightarrow \pi\pi$. The analytic model [45] predicts a decreasing cross section for this process with pion exchange reaching $< 10\%$ of the observed cross section at the peak of the f_2 . After inclusion of vector exchange, this contribution doubles. Because of form factor effects involved in the photon coupling to hadrons, these predictions from point like hadrons are to be taken rather as upper limits. This requires the need of “direct coupling” of $f_2 \rightarrow \gamma\gamma$. Indeed, it is well known that the radiative decays of the tensor mesons f_2, f_2', a_2 are well described by a model with direct coupling to the $q\bar{q}$ constituents according to the $SU(3)$ structure of the nonet with nearly ideal mixing (see e.g. Ref. [51]). Another example of a direct process is the production of ρ mesons in the process $\gamma p \rightarrow \pi^+\pi^-p$ by direct VMD coupling, which is found much larger than the rescattering contribution from the “Drell-Söding” background process [52]. We therefore interpret the direct terms in the $\gamma\gamma$ processes as representing the amplitudes with coupling of the photon to the partonic constituents of the resonances (such as $q\bar{q}, 4q, gg, \dots$).

4. Direct and rescattering couplings of the σ

In the application of the analytic model [45], we first obtain a suitable parametrisation of the $\pi\pi$ scattering data, and then determine the direct coupling by comparing the model with the $\gamma\gamma$ results. In the present paper, we restrict ourselves to the low mass region below 700 MeV where we neglect vector and axial-vector exchanges⁴, inelastic channels and D-waves, furthermore, we assume a pointlike pion-photon coupling.

Amplitude for elastic $\pi\pi$ scattering

In the K-matrix fits to the $\pi\pi$ elastic scattering data for the range of energy [(0.5-1.8) GeV], a pole is found in the isoscalar S-wave amplitude $T_0^{(0)}$ with a large imaginary part which corresponds to a state [53,54,55]:

$$M \approx \Gamma \approx 1 \text{ GeV}, \quad (1)$$

⁴They only start to be relevant above 700 MeV [45].

though this value may depend on the treatment of the other resonances [30,6,41]. The mass value in Eq. (1) is close to the one where the observed S-wave phase shift goes through 90° as in a simple Breit Wigner form without background. This broad object has been called $f_0(1000)$ [55], for a while $f_0(400 - 1200)$ by the PDG and now $f_0(600)/\sigma$. In general, the complex resonance self-energy $\Sigma = M - (i/2)\Gamma$ is energy dependent and determines the poles of the S-matrix corresponding to mass and width of the physical particles; they do not usually coincide with the Breit Wigner masses. In recent determinations, where analyticity and unitarity properties are used to continue the amplitude into the deep imaginary region, one obtains for the complex σ pole ⁵:

$$441 - i 272 \text{ MeV [56] or } 489 - i 264 \text{ MeV [57]}. \quad (2)$$

We shall see that the σ pole can be referred to the same broad object defined above. For applying the analytic model [45], we introduce a *shape function* $f_0(s)$ which multiplies the $\sigma\pi\pi$ coupling. For simplicity, we don't include the 4-point coupling term. The real analytic function $f_0(s)$ is regular for $s > 0$ and has a left cut for $s \leq 0$. For our low energy approach, a convenient approximation, which allows for a zero at $s = s_A$ and a pole at $\sigma_D > 0$ simulating the left hand cut, is:

$$f_0(s) = \frac{s - s_{A0}}{s + \sigma_{D0}}. \quad (3)$$

The unitary $\pi\pi$ amplitude is then written as:

$$T_0^{(0)}(s) = \frac{Gf_0(s)}{s_R - s - G\tilde{f}(s)} = \frac{Gf_0(s)}{\mathcal{D}(s)}. \quad (4)$$

$T_\ell^{(I)} = e^{i\delta_\ell^{(I)}} \sin \delta_\ell^{(I)} / \rho$ with $\rho(s) = (1 - 4m_\pi^2/s)^{1/2}$; $G = g_{\pi,B}^2$ is the bare coupling squared and:

$$\text{Im } \mathcal{D} = \text{Im}(-G\tilde{f}_0) = -(\theta\rho)G f_0, \quad (5)$$

with: $(\theta\rho)(s) = 0$ below and $(\theta\rho)(s) = \rho(s)$ above threshold $s = 4m_\pi^2$. The amplitude near the pole s_0 where $\mathcal{D}(s_0) = 0$ and $\mathcal{D}(s) \approx \mathcal{D}'(s_0)(s - s_0)$ is:

$$T_0^{(0)}(s) \sim \frac{g_\pi^2}{s_0 - s}; \quad g_\pi^2 = \frac{Gf_0(s_0)}{-\mathcal{D}'(s_0)}. \quad (6)$$

The real part of \mathcal{D} is obtained from a dispersion relation with subtraction at $s = 0$ and one obtains:

$$\tilde{f}_0(s) = \frac{2}{\pi} \left[h_0(s) - h_0(0) \right], \quad (7)$$

where: $h_0(s) = f_0(s)\tilde{L}_{s1}(s) - (\sigma_{N0}/(s + \sigma_{D0}))\tilde{L}_{s1}(-\sigma_{D0})$, σ_{N0} is the residue of $f_0(s)$ at $-\sigma_{D0}$ and: $\tilde{L}_{s1}(s) = [(s - 4m_\pi^2)/m_\pi^2]\tilde{L}_1(s, m_\pi^2)$ with \tilde{L}_1 from [45].

Amplitudes for $\gamma\gamma \rightarrow \pi\pi$ scattering

Starting from the S wave amplitude in Eq. (4) we derive the amplitude $T_\gamma^{(I)}$ for the electromagnetic process for isospin $I = 0$ as:

$$T_\gamma^{(0)} = \sqrt{\frac{2}{3}}\alpha \left(f_0^B + G \frac{\tilde{f}_0^B}{\mathcal{D}} \right) + \alpha \frac{\mathcal{P}}{\mathcal{D}}. \quad (8)$$

Here the contribution from the Born term of $\gamma\gamma \rightarrow \pi^+\pi^-$ is given by $f_0^B = 2L_1$ as defined in [45], a real analytic function in the s plane with left cut $s \leq 0$. The

function \tilde{f}_0^B represents $\pi\pi$ rescattering; it is regular for $s < 4m_\pi^2$ but has a right cut for $s \geq 4m_\pi^2$ with:

$$\text{Im } \tilde{f}_0^B(s + i\epsilon) = (\theta\rho f_0 f_0^B)(s), \quad (9)$$

which vanishes at $s = 0$. With this definition the Watson theorem is fulfilled, i.e. the phase of $T_\gamma^{(0)}$ is the same as the one of the elastic amplitude \mathcal{D}^{-1} in Eq. (4). The real part is derived from a dispersion relation with subtraction at $s = 0$ for \tilde{f}_0^B to satisfy the Thomson limit, and has a representation similar to the one in Eq. (7), but by replacing (\tilde{f}_0, h_0) by (\tilde{f}_0^B, h_0^B) . The function h_0^B is defined as h_0 below Eq. (7) but with \tilde{L}_1 replaced by $-\tilde{L}_1^2$ everywhere. It vanishes at $s = -\sigma_{D0}$ and $\tilde{f}_0^B(s)$ is regular at this point. Finally, the polynomial \mathcal{P} reflects the ambiguity from the dispersion relations and is set here to $\mathcal{P} = sF_\gamma\sqrt{2}$. It represents the direct coupling of the resonance to $\gamma\gamma$. The residues at the pole s_0 of the rescattering and direct contributions to $T_\gamma^{(0)}$ in Eq. (8), respectively, are obtained as:

$$g_\gamma^{\text{resc}} g_\pi = \sqrt{\frac{2}{3}}\alpha \frac{G\tilde{f}_0^B(s_0)}{-\mathcal{D}'(s_0)}; \quad g_\gamma^{\text{dir}} g_\pi = \alpha \frac{s_0 F_\gamma \sqrt{2}}{-\mathcal{D}'(s_0)}, \quad (10)$$

from which one can deduce the branching ratio:

$$\frac{\Gamma_{\sigma \rightarrow \gamma\gamma}}{\Gamma_{\sigma \rightarrow \pi\pi}} \simeq \frac{1}{|\rho(s_0)|} \left| \frac{g_\gamma}{g_\pi} \right|^2 \simeq \frac{2\alpha^2}{|\rho(s_0)|} \left| \frac{s_0}{Gf_0(s_0)} \right|^2 F_\gamma^2. \quad (11)$$

Similarly, we parametrize the $I = 2$ S-wave amplitude $T_0^{(2)}$ by introducing the shape function f_2 :

$$T_0^{(2)} = \frac{\Lambda f_2(s)}{1 - \Lambda \tilde{f}_2(s)}, \quad f_2(s) = \frac{s - s_{A2}}{(s + \sigma_{D1})(s + \sigma_{D2})}, \quad (12)$$

and obtain:

$$T_\gamma^{(2)} = \frac{\alpha}{\sqrt{3}} \left(f_2^B + \frac{\Lambda \tilde{f}_2^B(s)}{1 - \Lambda \tilde{f}_2(s)} \right), \quad (13)$$

where $f_2^B = f_0^B$ and: $\text{Im}\tilde{f}_2(s) = (\theta\rho)f_2(s)$, $\text{Im}\tilde{f}_2^B(s) = (\theta\rho f_2 f_2^B)(s)$. These amplitudes are again both subtracted at $s = 0$ as in case of $I = 0$ and one finds in analogy:

$$\tilde{f}_2(s) = \frac{2}{\pi} \left[h_2(s) - h_2(0) \right], \quad (14)$$

where: $h_2(s) = f_2(s)\tilde{L}_{s1}(s) - (\sigma_{N1}/(s + \sigma_{D1}))\tilde{L}_{s1}(-\sigma_{D1}) - (\sigma_{N2}/(s + \sigma_{D2}))\tilde{L}_{s1}(-\sigma_{D2})$; σ_{N1}, σ_{N2} are the residues of $f_2(s)$ at $-\sigma_{D1}, -\sigma_{D2}$ and $\tilde{f}_2^B(s)$ is defined as $\tilde{f}_2(s)$ in Eq. (14) but with \tilde{L}_{s1} replaced by $-\tilde{L}_{s1}^2$. The cross sections for the $\pi\pi$ and $\gamma\gamma$ scattering processes are obtained from the previous expressions of the amplitudes as described in the Appendices of [45], where the $\cos\theta$ integration should be done from 0 to 1 for the neutral and from -1 to 1 for the charged cases ⁶.

Results of the analysis

The analytic model in its original parametrization [45] without direct term has given already quite a decent description of the data available now for both charge states $\pi^+\pi^-$ and $\pi^0\pi^0$ within $\sim 20\%$ as discussed previously [39]. This already indicates that the direct term is much smaller than the rescattering term. In the present analysis, we repeat the calculation but take the new version of the model [45] by introducing the *shape function* $f_0(s)$

⁵A similar result [see Eq. (17)] is found in the analytic model [45].

⁶The range of integration may have been misused in [58].

defined in Eq. (3). We first determine the parameters of the model for $\pi\pi$ scattering below 700 MeV from the best approximation of our formula to the phase shifts $\delta_0^{(0)}$ and $\delta_0^{(2)}$ obtained in the Roy equation analysis in [56], which takes into account the high-energy behaviour suggested in [57]. For $I = 0$, we obtain in units of GeV^2 :

$$\begin{aligned} s_{A0} &= 0.016, & G &\simeq 1.184, \\ s_R &= 0.823, & \sigma_{D0} &= 0.501, \end{aligned} \quad (15)$$

and for $I = 2$:

$$\begin{aligned} s_{A2} &= 0.039, & \Lambda &\simeq -4.136, \\ \sigma_{D1} &= 0.693, & \sigma_{D2} &= 4.384, \end{aligned} \quad (16)$$

from which, we find the pole mass and residue:

$$M_\sigma \simeq 422 - i 290 \text{ MeV}; \quad g_\pi \simeq 0.06 - i 0.50 \text{ GeV}, \quad (17)$$

which is close to the mass M_σ in Eq. (2) and in the previous paper [45]. Given the $\pi\pi$ amplitude we can predict the cross sections for $\gamma\gamma \rightarrow \pi\pi$ where the only free parameter F_γ is related to the strength of the direct coupling $\sigma \rightarrow \gamma\gamma$. The fit of the model involving both the $\pi\pi$ rescattering and direct meson couplings to the data from Crystal Ball ($\pi^0\pi^0$) [59] and MARK-II ($\pi^+\pi^-$) [60] collaborations is shown in Figs. 1 and 2 for the cases with and without direct contribution. A si-

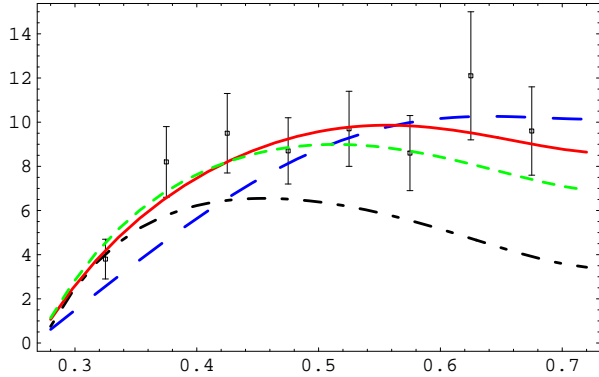


Figure 1. a) Fit of the $\pi^0\pi^0$ cross-section in nanobarn (nb) versus \sqrt{s} using unitarized Born amplitude: $F_\gamma = 0$ (dot-dashed); $F_\gamma = -0.09$: $I=0$ (large dashed), $I=0+2$ (continuous); $F_\gamma = -0.07$: $I=0+2$ (small dashed). The data are from Crystal Ball [59] for $|\cos\theta| \leq 0.8$;

multaneous best fit of the data in the region below 700 MeV, is obtained for : $F_\gamma \simeq -0.070$, at the minimum $\chi^2 \simeq 25.6$ (19 data points) in Fig. 2b) ⁷. However, a fit of the neutral channel alone gives a much better fit: $F_\gamma \simeq -0.090$, for a $\chi^2 = 3.38$ (8 data points) in Fig. 1b). In the charged channel, this is due to the deviations of the fit at high-mass; the large systematic errors and the absence of data points in the region 0.40 to 0.55 GeV do not permit a good understanding of this channel. One can notice that the $I = 2$ S -wave amplitude which reproduces with high-accuracy the CGL points [56] improves the agreement with the data in the neutral case

⁷ In the earlier analysis [45], a value F_γ of $\mathcal{O}(1)$ has been found, which corresponds to the DM2 data in [61] which are about twice the one of MARKII [60], i.e twice the Born contribution.

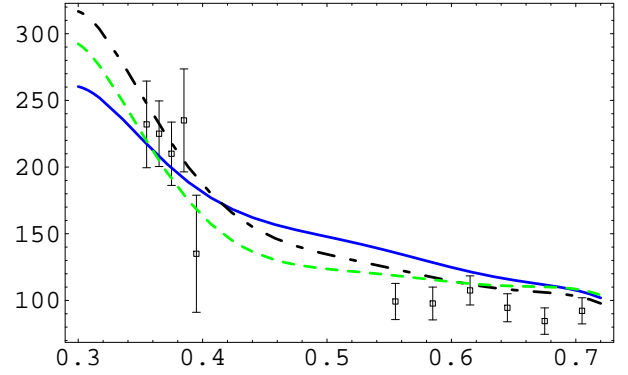


Figure 2. a) The same as in Fig. 1 but for $\pi^+\pi^-$ using unitarized Born amplitude: $F_\gamma = 0$ (dot-dashed); $F_\gamma = -0.07$ and $I=0+2$ (small dashed). The continuous line corresponds to the non-unitarized Born amplitude with $F_\gamma = 0$. The data are from MARKII [60] for $|\cos\theta| \leq 0.6$. versus F_γ .

(Fig. 1) but gives negligible contribution for the charged pion. For definiteness, we consider as a final estimate the mean value of the previous numbers:

$$F_\gamma \simeq -(0.080 \pm 0.014), \quad (18)$$

where we consider that the uncertainty in the fitting procedure 0.010 is expressed by this range. We have added linearly the systematics of the method to be about 5%, which we have estimated from the deviation of the mass and width determinations in Eq. (17) from the ones [56] in Eq. (2), as we have used their parametrization for fixing the parameters of the model. The corresponding values of the residues in units of $\alpha \times 10^{-3}$ GeV are:

$$\begin{aligned} g_\gamma^{\text{dir}} &\simeq (7 \pm 1) + i (31 \pm 4), \\ g_\gamma^{\text{resc}} &\simeq (90 + 5) + i (116 \pm 6). \end{aligned} \quad (19)$$

Using Eqs. (11, 17, 18) and $\Gamma_{\sigma \rightarrow \pi\pi} = 2\text{Im}M_\sigma$, we can deduce the “partial” $\gamma\gamma$ widths at the complex pole :

$$\begin{aligned} \Gamma_{\sigma \rightarrow \gamma\gamma}^{\text{dir}} &\simeq (0.13 \pm 0.05) \text{ keV}, \\ \Gamma_{\sigma \rightarrow \gamma\gamma}^{\text{resc}} &\simeq (2.7 \pm 0.4) \text{ keV}, \end{aligned} \quad (20)$$

and the total $\gamma\gamma$ width (direct + rescattering):

$$\Gamma_{\sigma \rightarrow \gamma\gamma}^{\text{tot}} \simeq (3.9 \pm 0.6) \text{ keV}, \quad (21)$$

Improvements of these estimates need more precise data below 700 MeV, and an extension of the analysis to higher energies.

Comparisons with existing results

Direct $\gamma\gamma$ width - Our result for the direct coupling is comparable with our previous value [39] obtained without using the shape function $f_0(s)$. In a parallel analysis [62], a K-matrix model analogous to Ref. [45] has been applied in a larger energy range of energy, including the recent BELLE data [63] and still assuming elementary pion and kaon exchange; a smaller direct coupling was obtained, but without error analysis.

Total $\gamma\gamma$ width - Our result is compatible with the range of values (1.2 ~ 3.2) keV obtained in [39] using a Breit-Wigner parametrization of the $\gamma\gamma \rightarrow \pi^0\pi^0$ data. It is also in the range of values based on dispersion relations (see introduction), though a direct comparison is difficult to do as these analyses are extended to higher

energy region, and we have an additional determination of the direct term. In our analysis below 700 MeV, we have also neglected the ω and axial-vector exchange in agreement with [45]. Other calculations find contributions of 2.5% [49] or 16% [37] at 400 MeV. One can notice that the effect of the direct term in our Fig. 1, distorts the shape of the unitarized Born curve, and then permits a good fit of all points below 700 MeV, which is not the case of the one in [37]. Then, if our fit was restricted to lower masses to suppress these other exchanges no different results are to be expected.

“On-shell” σ mass and widths

For a more appropriate comparison with QSSR predictions, one can introduce the mass and widths of the “visible meson” on the real axis. This can be either the Breit-Wigner mass and width in Eq. (1) or/and the “on shell” mass and widths (see e.g. [64]).

Mass of the σ - A Breit-Wigner parametrization of the data, leads to value given in Eq. (1): $M_\sigma^{\text{bw}} \approx \Gamma_\sigma^{\text{bw}} \approx 1$ GeV, which can be compared with the “on-shell mass” M_σ^{os} in the model [45] where the amplitude is purely imaginary at the phase 90° :

$$\text{Re}\mathcal{D}((M_\sigma^{\text{os}})^2) = 0 \implies M_\sigma^{\text{os}} \approx 0.92 \text{ GeV} . \quad (22)$$

Hadronic width - In the same way as for the mass, one can define an “on-shell width” [see Eqs. (5) and (6)] evaluated at $s = (M_\sigma^{\text{os}})^2$:

$$M_\sigma^{\text{os}} \Gamma_\sigma^{\text{os}} \simeq \frac{\text{Im } \mathcal{D}}{-\text{Re } \mathcal{D}} \implies \Gamma_{\sigma \rightarrow \pi\pi}^{\text{os}} \approx 1.02 \text{ GeV} , \quad (23)$$

to be compared with the Breit-Wigner width in Eq. (1).

Direct $\gamma\gamma$ width - As there are no separated S wave cross sections we use here only the estimates based on the analytic model [45] where we proceed as in the previous section but we evaluate the parameters at $s_0 = (M_\sigma^{\text{os}})^2$. Then, we obtain from Eq. (11):

$$\Gamma_{\sigma \rightarrow \gamma\gamma}^{\text{os,dir}} \approx (1.0 \pm 0.4) \text{ keV} . \quad (24)$$

As the model is extrapolated here towards energies beyond its validity, we expect that the previous results are a crude approximation and will only serve as a guideline.

5. QSSR/LET results and QCD tests of the σ

The QSSR/LET results obtained in the physical region can be better compared with experiment by using the result for a Breit-Wigner parametrization of the data in Eq. (1) or by using the results for the on-shell mass derived previously but not by directly comparing with the parameters of the complex pole. The direct $\gamma\gamma$ coupling, which can reveal the photon coupling to the intrinsic quark ($q\bar{q}$, $4q, \dots$) or/and gluon (gg, \dots) constituent internal structure of the resonance, can be also related to the QSSR and/or LET evaluations of its width through quark or gluon loops like is the case of the quark triangle for the pion and/or the $f_2(1270)$. As the comparison with QSSR/LET is an important step for interpreting our fitted values, it is essential to review shortly the main steps in the derivations of the results.

Gluonia masses from QSSR

Masses of the bare unmixed scalar gluonium can be determined from the two Laplace unsubtracted (USR) and

subtracted (SSR) sum rules:

$$\begin{aligned} \mathcal{L}_0(\tau) &= \frac{1}{\pi} \int_0^\infty dt e^{-t\tau} \text{Im}\psi(t) , \\ \mathcal{L}_{-1}(\tau) &= -\psi(0) + \frac{1}{\pi} \int_0^\infty \frac{dt}{t} e^{-t\tau} \text{Im}\psi(t) , \end{aligned} \quad (25)$$

of the two-point correlator $\psi(q^2)$ associated to the trace of the QCD energy-momentum tensor current:

$$\theta_\mu^\mu = \frac{1}{4} \beta(\alpha_s) G_{\mu\nu}^a G_a^{\mu\nu} + [1 + \gamma_m(\alpha_s)] \sum_{u,d,s} m_q \bar{\psi}_q \psi_q . \quad (26)$$

τ is the sum rule variable; $\beta(\alpha_s) \equiv \beta_1(\alpha_s/\pi) + \dots$ and $\gamma_m(\alpha_s) \equiv \gamma_1(\alpha_s/\pi) + \dots$ are the QCD β -function and quark mass anomalous dimension: $-\beta_1 = (1/2)(11 - 2n_f/3)$, $\gamma_1 = 2$ for $SU(3)_c \times SU(n_f)$. The subtraction constant $\psi(0) = -16(\beta_1/\pi) \langle \alpha_s G^2 \rangle$ expressed in terms of the gluon condensate [20] $\langle \alpha_s G^2 \rangle = (0.07 \pm 0.01) \text{ GeV}^4$ [65,26] affects strongly the USR analysis which has lead to apparent discrepancies in the previous literature when a single resonance is introduced into the spectral function [23]. The SSR being sensitive to the high-energy region ($\tau \simeq 0.3 \text{ GeV}^{-2}$) predicts [4]:

$$M_G \simeq (1.5 \sim 1.6) \text{ GeV} , \quad (27)$$

comparable with the quenched lattice value [18], while the USR stabilizes at lower energy ($\tau \simeq 0.8 \text{ GeV}^{-2}$) and predicts a low-mass gluonium [22]:

$$M_{\sigma_B} \simeq (0.95 \sim 1.10) \text{ GeV} , \quad (28)$$

comparable with the unquenched lattice value [19]. Furthermore, the consistency of the USR and SSR can be achieved by a two-resonances (G and σ) + “QCD continuum” parametrization of the spectral function [24]⁸.

Gluonia couplings to Goldstone boson pairs

These couplings can be obtained from the vertex function:

$$V[q^2 \equiv (q_1 - q_2)^2] \equiv \langle \pi_1 | \theta_\mu^\mu | \pi_2 \rangle , \quad (29)$$

obeying a once subtracted dispersion relation:

$$V(q^2) = V(0) + q^2 \int_{4m_\pi^2}^\infty \frac{dt}{t} \frac{1}{t - q^2 - i\epsilon} \frac{1}{\pi} \text{Im}V(t) . \quad (30)$$

with the condition: $V(0) = \mathcal{O}(m_\pi^2) \rightarrow 0$ in the chiral limit. Using also the fact that $V'(0) = 1$, one can then derive the two sum rules:

$$\frac{1}{4} \sum_{S=\sigma_B, \dots} g_{S\pi\pi} \sqrt{2} f_S = 0 , \quad \frac{1}{4} \sum_{S=\sigma_B, \dots} g_{S\pi\pi} \frac{\sqrt{2} f_S}{M_S^2} = 1 , \quad (31)$$

where f_S is the decay constant analogue to f_π . The 1st sum rule requires the existence of at least two resonances coupled strongly to $\pi\pi$. Considering the σ_B and σ'_B but neglecting the small G -coupling to $\pi\pi$ as indicated by GAMS [66]⁹, one predicts in the chiral limit [24,4]:

$$|g_{\sigma_B \pi^+ \pi^-}| \simeq |g_{\sigma_B K^+ K^-}| \simeq (4 \sim 5) \text{ GeV} , \quad (32)$$

⁸In [4] the QCD continuum has also been modeled by a σ'_B (radial excitation of the σ_B), which enables to fix the decay constant f_{σ_B, σ'_B} once the σ_B, σ'_B masses are introduced as input.

⁹The $G(1.6)$ is expected to couple mainly to the $U(1)_A$ channels $\eta'\eta'$ and through mixing to $\eta\eta', \eta\eta$ [24,4].

a universal coupling, which will imply a large width ¹⁰:

$$\Gamma_{\sigma_B \rightarrow \pi^+ \pi^-} \equiv \frac{|g_{\sigma_B \pi^+ \pi^-}|^2}{16\pi M_{\sigma_B}} \left(1 - \frac{4m_\pi^2}{M_{\sigma_B}^2}\right)^{1/2} \simeq 0.7 \text{ GeV}. \quad (33)$$

This large width into $\pi\pi$ is a typical OZI-violation due to non-perturbative effects expected to be important in the region below 1 GeV, where perturbative arguments valid in the region of the $G(1.5-1.6)$ cannot be applied. This result can be tested using lattice calculations with dynamical fermions.

Gluonia couplings to $\gamma\gamma$

These couplings can be derived by identifying the Euler-Heisenberg effective Lagrangian for $gg \rightarrow \gamma\gamma$ via a quark constituent loop to the scalar one: $\mathcal{L}_{S\gamma\gamma} = g_{S\gamma\gamma} S F_{\mu\nu}^{(1)} F_{\mu\nu}^{(2)}$, which leads to the sum rule ¹¹:

$$g_{S\gamma\gamma} \simeq \frac{\alpha}{60} \sqrt{2} f_S M_S^2 \left(\frac{\pi}{-\beta_1}\right) \sum_{q=u,d,s} Q_q^2 / M_q^4, \quad (34)$$

where Q_q is the quark charge in units of e ; $M_{u,d} \approx M_\rho/2$ and $M_s \approx M_\phi/2$; are constituent masses; S refers to gluonium (σ_B, \dots). Then, one predicts the couplings:

$$g_{\sigma_B \gamma\gamma} \approx g_{\sigma'_B \gamma\gamma} \simeq g_{G\gamma\gamma} \simeq (0.4 \sim 0.7) \alpha \text{ GeV}^{-1}, \quad (35)$$

and the corresponding widths ¹²:

$$\Gamma_{\sigma_B \rightarrow \gamma\gamma} \equiv \frac{|g_{\sigma_B \gamma\gamma}|^2}{16\pi} M_{\sigma_B}^3 \simeq (0.2 \sim 0.6) \text{ keV}. \quad (36)$$

For a self-consistency check of the previous results, one can introduce their values into the sum rule:

$$\frac{1}{4} \sum_{S=\sigma_B, \dots} g_{S\gamma\gamma} \sqrt{2} f_S = \frac{\alpha R}{3\pi}, \quad (37)$$

where $R \equiv 3 \sum Q_q^2$, derived [28,31] from $\langle 0 | \theta_\mu^\mu | \gamma_1 \gamma_2 \rangle$, by matching the k^2 dependence of its two sides.

QCD tests of the $\sigma/f_0(600) = \text{a gluonium?}$

One can notice that the QSSR and LET predictions for the mass, hadronic and electromagnetic widths of a low mass gluonium σ_B are in remarkable agreement with previous results from $\pi\pi$ and $\gamma\gamma$ scatterings for an on-shell or/and Breit-Wigner resonance. However, the fitted value of direct width in Eq. 24 to $\gamma\gamma$ needs to be improved for a sharper comparison. This ‘‘overall agreement’’ favours a large gluon component in the $\sigma/f_0(600)$ wave function. Its large width into $\pi\pi$ indicates a strong violation of the OZI rule in this channel and signals large non-perturbative effects in its treatment. This large hadronic width also disfavours its $\bar{q}q$ interpretation. In fact QSSR predicts for a $S_2 \equiv (\bar{u}u + \bar{d}d)$, with mass of 1 GeV, a $\pi^+ \pi^-$ width of about (120 \sim 180) MeV [3,4,7]¹³, and a $S_2 \rightarrow \gamma\gamma$ width of about 5 keV. The later can be deduced by using the quark charge squared

relation (25/9) with $\Gamma_{a_0 \rightarrow \gamma\gamma} \approx 2 \text{ keV}$, obtained from the quark triangle loop including the $\langle \bar{\psi}\psi \rangle$ condensate contribution [13]. In the same way, QSSR also predicts, for a four-quark state, having the same mass of 1 GeV [12,13], a $\gamma\gamma$ width of about 0.4 eV [13]. Both $\bar{q}q$ and 4-quark scenarios are disfavoured by the value of the direct coupling fitted from $\gamma\gamma$ scattering.

6. Summary and conclusions

We have reanalyzed the $\pi\pi$ and $\gamma\gamma$ scattering data in the mass region below 700 MeV. We applied an analytic K -matrix model which is based on an effective theory with couplings between resonances, hadrons and photons. The model around the threshold region resembles in its structure with Chiral Perturbation Theory, while the inclusion of resonances and a resummation of a class of meson loop corrections permit its applications towards higher energies. Then, the two-photon decay of a resonance can proceed either through intermediate decay into hadrons and subsequent annihilation or through the direct transition. The low energy processes considered here are dominated in our fits by the $f_0(600)/\sigma$ resonance. Its total radiative width of about 4 keV is dominated by the rescattering component which is uniquely predicted for known elastic $\pi\pi$ scattering. The direct coupling width is found an order of magnitude smaller (0.13 keV). It can be interpreted as representing its intrinsic quark ($q\bar{q}$, $4q, \dots$) or/and gluon (gg, \dots) constituent contribution to the $\gamma\gamma$ width.

A confrontation of the overall fitted resonance parameters with the QSSR predictions reviewed in Section 5, for an unmixed bare gluonium σ_B having a mass about 1 GeV, indicate that the $\sigma/f_0(600)$ can contain a large gluon component in its wave function. A light glueball/gluonium near 1 GeV is also suggested from lattice QCD calculations including dynamical fermions and from the phenomenological analysis of the scalar meson spectrum.

It will be interesting to extend this analysis towards higher energies where new channels ($K\bar{K}$) will be opened and some other resonances will show up. This allows for additional constraints on our approach and possible tests of the gluon/quark structure of $\sigma/f_0(600)$.

Acknowledgements

We thank Peter Minkowski for the collaboration in an earlier phase of this work. One of us (W.O.) would like to thank Stephan Narison for the invitation and for the kind hospitality at the Montpellier University within the grant provided by Region of Languedoc-Roussillon Septimanie where this work had begun.

¹⁰However, the analysis in Ref. [4] also indicates that σ_B having a mass below 750 MeV cannot be wide ($\leq 200 \text{ MeV}$) (see also some of Ref. [23]) due to the sensitivity of the coupling to M_σ . Wide low-mass gluonium has also been obtained using QSSR (1st ref. in [23]), an effective Lagrangian [31] and LET [27].

¹¹This sum rule has been used in [27] for the charm quark.

¹²Due to their M^3 -dependence, the widths of the σ'_B and G can be much larger: (0.4 \sim 2) keV. These widths induce a tiny effect of $(3-9) \times 10^{-11}$ to the muon ($g-2$) [67] and cannot be excluded.

¹³The 1st result in [68] contains an unfortunate numerical error.

REFERENCES

1. For reviews, See e.g.: L. Montanet, *Nucl. Phys. Proc. Suppl.* **86**, (2000) 381; U. Gastaldi, *Nucl. Phys. Proc. Suppl.* **96**, (2001) 234; E. Klempt and A. Zaitsev, *Phys. Rep.* **454** (2007) 1.
2. D. Morgan, *Phys. Lett.* **B 51** (1974) 71.
3. A. Bramon and S. Narison, *Mod. Phys. Lett.* **A 4** (1989) 1113.
4. S. Narison, *Nucl. Phys.* **B 509** (1998) 312; *Nucl. Phys. Proc. Suppl.* **64** (1998) 210; *Nucl. Phys. Proc. Suppl.* **96** (2001) 244.
5. E. Klempt, B.C. Metsch, C.R. Münz and H.R. Petry, *Phys. Lett.* **B 361** (1995) 160.
6. P. Minkowski and W. Ochs, *Eur. Phys. J.* **C 9** (1999) 283.
7. S. Narison, *Phys. Rev.* **D 73** (2006) 114024.
8. N. Tornqvist, *Phys. Rev. Lett.* **49** (1982) 624; *Z. Phys.* **C 68** (1995) 467.
9. E. van Beveren et al., *Z. Phys.* **C 30** (1986) 615; E. van Beveren and G. Rupp, *Eur.Phys.J.* **C 10** (1999) 469.
10. R. Jaffe, *Phys. Rev.* **D 15** (1977) 267; *Phys. Rev.* **D 15** (1977) 281.
11. J.M. Richard, *Nucl. Phys. Proc. Suppl.* **164** (2005) 131; D. Black et al., *Phys. Rev.* **D 59** (1999) 074026; A. Fariborz, J. Schechter, *Phys. Rev.* **D 60** (1999) 034002; D. Wong and K.F. Liu, *Phys. Rev.* **D 21** (1980) 2039; M. Alford and R.L. Jaffe, *Nucl. Phys.* **B 509** (1998) 312; F. Buccella et al., *Eur. Phys. J.* **C 49** (2007) 743; M. Karliner, H. J. Lipkin, *Phys. Lett.* **B 612** (2005) 197; L. Maiani et al., *Phys. Rev. Lett.* **93** (2004) 212002; A. Selem and F.Wilczek, hep-ph/0602128.
12. J.I. Latorre and P. Pascual, *Jour. Phys.* **G 11** (1985) L231; T.V. Brito et al., *Phys. Lett.* **B 608** (2005) 69; R.D. Matheus et al., *Phys. Rev.* **D 76** (2007) 056005.
13. S. Narison, *Phys. Lett.* **B 175** (1986) 88.
14. N.N. Achasov, S.A. Devyanin and G.N. Shestakov, *Z. Phys.* **C 16** (1984) 55; C. Hanhart et al., hep-ph / 0701214.
15. N. Isgur and J. Weinstein, *Phys. Rev.* **D 41** (1990) 2236.
16. T. Barnes, *Phys. Lett.* **B 165** (1985) 434; Proc. IXth Int. Workshop on $\gamma\gamma$ collisions, World Scientific (1992) 263 ed. D. Caldwell and H.P. Paar.
17. G. Janssen et al., *Phys. Rev.* **D 52** (1995) 2690.
18. C. Morningstar and M. J. Peardon, *Phys. Rev.* **D 60** (1999) 034509; G. Bali et al., *Phys. Rev.* **D 62** (2000) 054503; A. Hart and M. Teper, *Phys. Rev.* **D 65** (2002) 34502; Y. Chen et al., *Phys. Rev.* **D 74** (2006) 094005; ; H. Wada et al., *Phys. Lett.* **B 652** (2007) 250.
19. A. Hart et al., *Phys. Rev.* **D 74** (2006) 114504; T. Kunihiro et al., *Phys. Rev.* **D 70** (2004) 034504.
20. V.A. Novikov et al., *Nucl. Phys.* **B 191** (1981) 301.
21. K. Chetyrkin, S. Narison and V.I. Zakharov, *Nucl. Phys.* **B 550** (1999) 353.
22. S. Narison, *Z. Phys.* **C 26** (1984) 209.
23. P. Pascual and R. Tarrach, *Phys. Lett.* **B 113** (1982) 495; S. Narison, *Phys. Lett.* **B 125** (1983) 501; C.A. Dominguez and N. Paver, *Z. Phys.* **C 31** (1986) 591; J. Bordes, V. Gimenez and J.A. Peñarrocha, *Phys. Lett.* **B 223** (1989) 251; E. Bagan and T.G. Steele, *Phys. Lett.* **B 243** (1990) 413; J.L. Liu and D. Liu, *J. Phys* **G 19** (1993) 373; L.S. Kisslinger, J. Gardner and C. Vanderstraeten, *Phys. Lett.* **B 410** (1997) 1; T. Huang, H.Y. Jin and A.L. Zhang, *Phys. Rev.* **D 58** (1998) 312; T.G. Steele, D. Harnett and G. Orlandini, *AIP Conf. Proc.* **688** (2004) [hep-ph/0308074]; H. Forkel, *Phys. Rev.* **D 71** (2005) 054008.
24. S. Narison and G. Veneziano, *Int. J. Mod. Phys.* **A 4** (1989) 2751.
25. M.A. Shifman, A.I. Vainshtein and V.I. Zakharov, *Nucl. Phys.* **B 147** (1979) 385, 448.
26. For reviews, see e.g.: S. Narison, *Cambridge Monogr. Part. Phys. Nucl. Phys. Cosmol.* **17** (2004) 1-778 [hep-ph/0205006]; S. Narison, *World Sci. Lect. Notes Phys.* **26** (1989) 1-527; S. Narison, *Acta Phys. Pol.* **B 26** (1995) 687; S. Narison, *Riv. Nuovo Cim.* **10 N2** (1987) 1; S. Narison, *Phys. Rept.* **84** (1982) 263.
27. V.A. Novikov et al., *Nucl. Phys.* **B 165** (1980) 67.
28. R.J. Crewther, *Phys. Rev. Lett.* **28** (1972) 1421; J. Ellis and M.S. Chanowitz, *Phys. Lett.* **B 40** (1972) 397; *Phys. Rev.* **D 7** (1973) 2490.
29. C. Amsler and F.E. Close, *Phys. Rev.* **D 53** (1996) 295; D. Weingarten, *Nucl. Phys. Proc. Suppl.* **73** (1999) 283; F.E. Close and A. Kirk, *Eur.Phys.J.* **C 21** (2001) 531; F. Giacosa et al., *Phys. Lett.* **B 622** (2005) 277; X.G. He et al., *Phys. Rev.* **D 73** (2006) 114026.
30. V. Anisovich, Yu. Prokoshkin and A. Sarantsev, *Phys. Lett.* **B 389** (1996) 388.
31. J. Ellis and J. Lanik, *Phys. Lett.* **B 150** (1985) 289; *Phys. Lett.* **B 175** (1986) 83; J.Lanik, *Z. Phys.* **C 39** (1988) 143.
32. P. Di Vecchia and G. Veneziano, *Nucl. Phys.* **B 171** (1980) 253; P. Jain, R. Johnson and J. Schechter, *Phys. Rev.* **D 35** (1987) 2230.
33. L. Y. Xiao, H. Q. Zheng and Z. Y. Zhou, *Nucl. Phys. Proc. Suppl.* **174** (2007) 142.
34. G. Ecker et al., *Nucl. Phys.* **B321** (1989) 31.
35. M.R. Pennington, *Phys. Rev. Lett.* **97** (2006)011601 and *Mod. Phys. Lett.* **A 22** (2007) 1439; M. Boglione and M.R. Pennington, *Eur.Phys.J.* **C9** (1999) 11.
36. M.R. Pennington et al., arXiv:0803.3389 [hep-ph]
37. J.A. Oller, L. Roca and C. Schat, *Phys. Lett.* **B 659** (2008) 201; J.A. Oller and L. Roca, archiv:0804.0309 [hep-ph] (2008).
38. J. Bernabeu and J. Prades, *archiv:* 0802.1830 [hep-ph] (2008).
39. G. Mennessier, P. Minkowski, S. Narison, W. Ochs, SLAC Econf C0709107, arXiv:0707.4511 [hep-ph]
40. H. Fritzsch and P. Minkowski, *Nuovo Cimento* **A 30**

- (1975) 393.
41. W. Ochs, *Nucl. Phys. Proc. Suppl.* **174** (2007) 146.
 42. P. Minkowski and W. Ochs, *Nucl. Phys. Proc. Suppl.* **121** (2003) 119; *ibid* **121** (2003) 121.
 43. P. Minkowski and W. Ochs, *Eur. Phys. J. C* **39** (2005) 71.
 44. R. Omnes, *Nuov. Cim.* **8** (1958) 316; N.I. Muskhelishvili, "Singular integral equations", Amsterdam, North Holland 1958.
 45. G. Mennessier, *Z. Phys.* **C 16** (1983) 241.
 46. O. Babelon et al., *Nucl. Phys.* **B 113** (1976) 445; G. Mennessier and T.N. Truong, *Phys. Lett.* **B 177** (1986) 195. A Pean, Thèse Montpellier (1992) (unpublished).
 47. R.L. Goble, R. Rosenfeld and J.L. Rosner, *Phys. Rev.* **D39** (1989) 3264.
 48. J.F. Donoghue, B.R. Holstein and Y.C. Lin, *Phys. Rev.* **D 37** (1988) 2423; J.F. Donoghue and B.R. Holstein, *Phys. Rev.* **D 48** (1993) 137; J. Bijnens and F. Cornet, *Nucl. Phys.* **B 296** (1988) 557; L.V. Fil'kov, V.L. Kashevarov, *Phys. Rev.* **C 73** (2006) 035210.
 49. S. Bellucci, J. Gasser and M.E. Sainio, *Nucl. Phys.* **B 423** (1994) 80, Erratum-*ibid.* **B431** (1994) 413; M. Knecht, B. Moussallam, *J. Stern Nucl. Phys.* **B 429** (1994) 125.
 50. H.-J. Behrend, *Z. Phys.* **C56** (1992) 381.
 51. ARGUS Coll., H. Albrecht et al., *Z.Phys.C* **48** (1990) 183.
 52. J. Ballam et al., *Phys. Rev.* **D5** (1972) 545.
 53. B. Hyams et al., *Nucl. Phys.* **B 64** (1973) 134; G. Grayer et al., *Nucl. Phys.* **B 75** (1974) 189.
 54. P. Estabrooks, *Phys. Rev.* **D 19** (1979) 2678.
 55. K.L. Au, D. Morgan and M. Pennington, *Phys. Rev.* **D 35** (1987) 1633.
 56. I. Caprini, G. Colangelo and H. Leutwyler, *Phys. Rev. Lett.* **96** (2006) 132001.
 57. F.J. Yndurain, R. Garcia-Martin and J.R. Pelaez, *Phys. Rev.* **D 76** (2007) 074034.
 58. J. Harjes, Thesis, Univ. Hamburg, DESY Internal Report DESY FCE-91-01 (1991).
 59. H. Marsiske et al., Crystal Ball collaboration, *Phys. Rev.* **D 41** (1990) 3324.
 60. J. Boyer et al., MARK II Collaboration, *Phys. Rev.* **D42** (1990) 1350.
 61. A. Coureau et al., DM2 collaboration, *Phys. Lett.* **B 96** (1980) 402; Ch. Berger et al., PLUTO collaboration, *Phys. Lett.* **B 94** (1980) 254; R. Brandelik et al., TASSO collaboration, *Z. Phys.* **C 10** (1981) 117.
 62. N.N. Achasov and G.N. Shestakov, *Phys. Rev.* **D 77** (2008) 074020.
 63. K. Abe et al., BELLE collaboration, *arXiv:* 0711.1926 [hep-ex] (2007); T. Mori et al., *J. Phys. Soc. Jap.* **76** (2007) 074102.
 64. B.A. Kniehl and A. Sirlin, *arXiv:*0801.0669 [hep-ph] (2008).
 65. G. Launer, S. Narison, R. Tarrach, *Z. Phys* **C 26** (1984) 433; S. Narison, *Phys. Lett.* **B 387** (1996) 162.
 66. D. Alde et al., *Eur. Phys. J. A3* (1998) 361.
 67. S. Narison, *Phys. Lett.* **B 568** (2003) 231.
 68. G. Mennessier, S. Narison and N. Paver, *Phys. Lett.* **B 158** (1985) 153.